PHYSICAL REVIEW A

GENERAL PHYSICS

THIRD SERIES, VOL. 3, NO. 4 APRIL 1971

Quadratic Stark Effect in the $^2P_{3/2}$ States of the Alkali Atoms*

Robert W. Schmieder† and Allen Lurio‡
IBM Watson Laboratory, Columbia University, New York, New York 10025

and

W. Happer
Columbia University, New York, New York 10027
(Received 19 August 1970)

The method of pure electric field level-crossing spectroscopy has been used to measure the tensor polarizability of the $5^2P_{3/2}$ state of potassium. Our result is $\alpha_2 = -0.263(40)$ MHz/(kV/cm)^2. Numerical values of the scalar and tensor polarizabilities of the first, second, and third $^2P_{3/2}$ states of Li, Na, K, Rb, and Cs have been calculated using the Bates-Damgaard technique to evaluate the necessary radial integrals. The polarizabilities show remarkable systematic trends among the various states of the atoms. Our present and previously reported results are compared with previous theoretical and experimental work. The agreement between theoretical and experimental values ranges from fair to excellent.

I. INTRODUCTION

If an atom is placed in a small uniform electric field $\mathcal{E}$, the energy of the mth sublevel of the atom will be shifted by an amount $\Delta E(m)$ which is proportional to the square of the electric field.[1] One can write this Stark shift of the sublevel m as

$$\Delta E(m) = -\tfrac{1}{2}\alpha(m)\,\mathcal{E}^2 \quad . \tag{1}$$

The constant of proportionality $\alpha(m)$ is just the static electric polarizability of the atom in the sublevel m. The $2J+1$ polarizabilities of an atomic state of angular momentum J are not all independent,[2] since, regardless of the size of J, they can be expressed as linear combinations of a scalar polarizability α_0 and a tensor polarizability α_2:

$$\alpha(m) = \alpha_0 + \alpha_2\,[3m^2 - J(J+1)]/J(2J-1) \quad . \tag{2}$$

Equations (1) and (2) provide an adequate description of the Stark shifts which were observed in our work. A discussion of higher-order effects can be found in the work of Khadjavi *et al.*[3] The polarizabilities are of considerable interest since they can be expressed as linear combinations of the oscillator strengths of the atom. Thus, accurate values of the atomic polarizabilities can be used to check the consistency of experimental oscillator strengths. Also, in recent years Schwartz[4] and Dalgarno[5] have developed new methods, not based on perturbation theory, for computing Stark shifts.

The Stark effect in alkali atoms is especially interesting since the theoretical computation of the polarizability of an atom with a single valence electron is particularly straightforward. Also, extensive experimental oscillator strengths are available for alkali atoms. Our interest in this paper is limited to the $^2P_{3/2}$ states of alkali atoms since only these states can be investigated by our experimental technique of electric field level-crossing spectroscopy. Excellent measurements of the Stark shifts in the $^2P_{3/2}$ states were made spectroscopically many years ago by Yao,[6] Kopfermann and Paul,[7] and Grotrian and Ramsauer.[8] More recently, Marrus and Yellin,[9] and Marrus, McColm, and Yellin[10] have used the atomic-beam technique to measure polarizabilities in the first ^2P states of K, Rb, and Cs. Khadjavi, Lurio, and Happer[3] used pure electric field level crossing to measure the tensor polarizability in the second $^2P_{3/2}$ states of Rb and Cs. Murakawa and Yamamoto[11] calculated shifts for the lowest P states of all the alkalis and for the second-lowest P state of cesium.

In this paper we report a new measurement of the tensor polarizability of the $5^2P_{3/2}$ state of potassium and we report new calculations of the scalar and tensor polarizabilities of the first, second, and

third $^2P_{3/2}$ states of Li, Na, K, Rb, and Cs.

II. THEORY OF STARK EFFECT IN THE ALKALI $^2P_{3/2}$ STATE

The computation of the quadratic Stark shifts is a straightforward application of second-order perturbation theory, and was performed many years ago by Kirkwood[12] and by Condon.[13] This approach is summarized by Condon and Shortley.[14] More recently, Angel and Sandars[2] and Khadjavi, Lurio, and Happer[3] have used the algebra of irreducible spherical tensors to elucidate the symmetry properties of the Stark effect. This approach allows easy separation of the effective Hamiltonian into a monopolelike and a quadrupolelike part with which are identified the scalar and tensor polarizabilities, respectively. This technique was used by Khadjavi *et al.*,[3] and we shall briefly review it here.

A. Hamiltonian

The interaction of an atom and a static uniform electric field $\vec{\mathcal{E}}$ is described by the operator

$$V = -\vec{\mathcal{E}} \cdot \vec{\mathcal{P}} \quad , \tag{3}$$

where $\vec{\mathcal{P}} = e\sum_i \vec{r}_i$ is the electric dipole moment operator. Since $\vec{r}_i$ has nonzero matrix elements only between states of opposite parity, the average value of V in any parity eigenstate vanishes. Hence, the change in energy of a state m, to lowest order in $\vec{\mathcal{E}}$, is given by the second-order perturbation formula

$$\Delta E(m) = \left\langle m \left| \sum_i \frac{\vec{\mathcal{E}} \cdot \vec{\mathcal{P}} \,|i\rangle\langle i|\, \vec{\mathcal{E}} \cdot \vec{\mathcal{P}}}{E(m) - E(i)} \right| m \right\rangle = \langle m | \mathcal{H}' | m \rangle , \tag{4}$$

where the sum extends over all intermediate states i of the atom. From (4) we see that the energy shift can be regarded as the diagonal matrix element of the effective Hamiltonian operator $\mathcal{H}'$. One can use the algebra of spherical tensors[2,3] to show that for a state of electronic angular momentum J and for an electric field along the z axis, the effective Hamiltonian is

$$\mathcal{H}' = -\tfrac{1}{2}\alpha_0 \mathcal{E}^2 - \tfrac{1}{2}\alpha_2 \mathcal{E}^2 \left[3J_z^2 - J(J+1)\right]/J(2J-1) . \tag{5}$$

Here α_0 and α_2 are the scalar and tensor polarizabilities of the atom.

The effective Hamiltonian may be regarded as a first-order perturbation within the sublevels of the atomic state J. Since the atomic sublevels are also perturbed by the interaction $\mathcal{H}_{hfs}$ between the atomic electrons and the nucleus, the energies and eigenstates of the atom are just the eigenvalues and eigenvectors of the Hamiltonian operator

$$\mathcal{H} = \mathcal{H}_{hfs} + \mathcal{H}' \quad . \tag{6}$$

The hyperfine interaction $\mathcal{H}_{hfs}$ can be expressed to sufficient accuracy in terms of the magnetic dipole and electric quadrupole coupling constants a and b:

$$\mathcal{H}_{hfs} = a\, I \cdot J + b\, \frac{3(I\cdot J)^2 + \frac{3}{2}(I\cdot J) - I(I+1)J(J+1)}{2I(2I-1)J(2J-1)} . \tag{7}$$

In diagonalizing (6) one can ignore the scalar component of the effective Hamiltonian (5) since this simply shifts all energy levels of the atomic multiplet by the same amount.

B. Breit Formula

Our experimental work made use of level-crossing spectroscopy. Details of the experimental method can be found in an earlier paper by Khadjavi *et al.*[3] The experiments are based on the fact that if atoms are excited by resonant light of polarization vector $\vec{f}$, the intensity of fluorescently scattered light of polarization vector $\vec{g}$ is given by the Breit formula

$$R(\vec{f}, \vec{g}) = C \sum \frac{f_{\mu m} f_{m\mu'} g_{\mu' m'} g_{m'\mu}}{1 + 2\pi i \tau \nu(\mu\mu')} \quad . \tag{8}$$

Here $f_{\mu m} = \langle \mu | \vec{f} \cdot \vec{p} | m \rangle$, etc., where $|\mu\rangle$ and $|m\rangle$ are excited-state and ground-state eigenvectors, respectively; τ is the radiative lifetime of the excited state, and

$$\nu(\mu\mu') = [E(\mu) - E(\mu')]/h \quad .$$

The excited-state energies $E(\mu)$ are the eigenvalues of the Hamiltonian (6). The factor C is proportional to the intensity of the exciting light. The summation in (12) extends over the indices m, m', μ, and μ'. Because of the dipole matrix elements $f_{\mu m}$, etc., the azimuthal quantum numbers associated with μ and μ' can differ by no more than 2 if the numerator of (8) is to be nonzero.

From (8) it is evident that resonant changes in the intensity of scattered light may occur whenever the frequency $\nu(\mu\mu')$ passes through zero, that is, whenever two energy levels cross. Since the scalar polarizability does not affect the frequencies $\nu(\mu\mu')$, a level-crossing experiment yields no information about α_0.

In practice, the intensity of fluorescent light is carefully measured as a function of the applied electric field. Values of the unknown atomic polarizability are then chosen to ensure the closest possible agreement between experimentally measured and theoretically predicted fluorescent intensities.

The Breit formula was evaluated by means of a computer program[3] and typical results for the energy levels are shown in Figs. 1–3. In these plots we have used the best values of a and b available. For α_2 we used the results of a Bates-Damgaard-(BD)-type calculation,[15] described in Sec. II C; (these values listed in Table III). The α_2 values

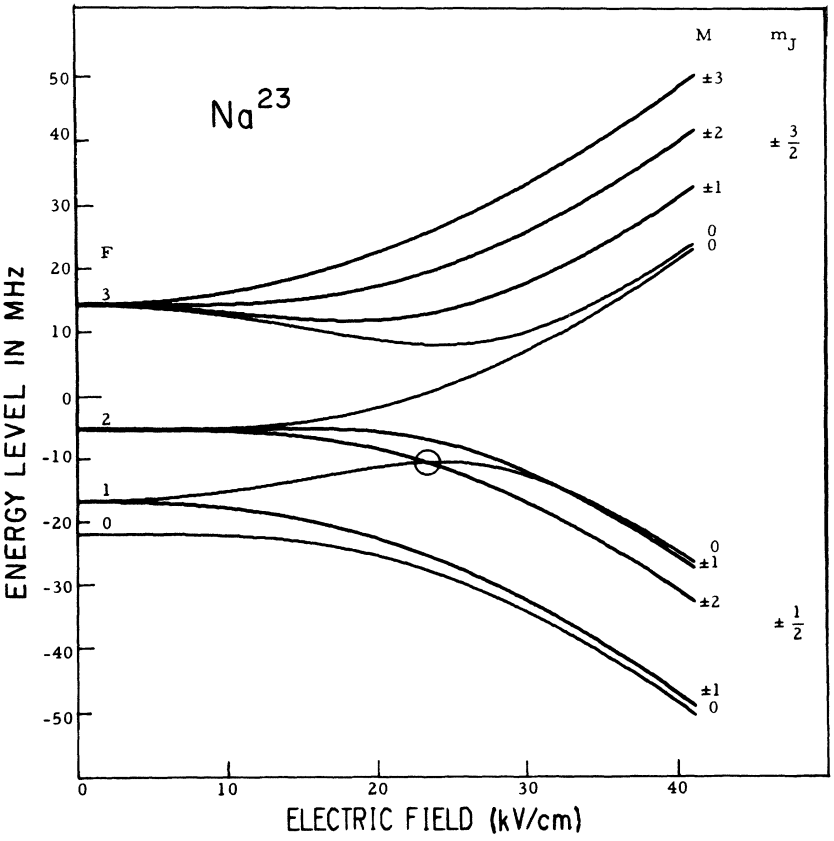

FIG. 1. Calculated energy levels for the $4\,^2P_{3/2}$ state of Na^{23} vs $\mathcal{E}$. A shift of the center of gravity of the energy levels has been suppressed. The hfs constants are taken as $a = 6.1$ MHz, $b = 1.0$ MHz. The tensor polarizability is taken as $\alpha_2 = -0.042$ MHz/(kV/cm)^2, which is the result of our BD calculation. The same plot is valid for the $3\,^2P_{3/2}$ state if the vertical scale is multiplied by 3.05 and the horizontal scale by $0.042/0.021 \simeq 2.3$.

are probably accurate to a few percent, judging by the agreement with the measurements that have been made to date.

An interesting aspect of Figs. 1–3 is that level crossings occur at nonzero values of $\mathcal{E}$. There are, of course, the zero-field crossings that are responsible for the electric field Hanle effect, but the high-field crossings are important because they will give additional structure to the level-crossing signals. The scalar energy shift $-\frac{1}{2}\alpha_0\mathcal{E}^2$ has not been included in the figures since the level-crossing signals are not affected by this common shift of all the atomic sublevels. Normally, $\alpha_0 > 0$, so there is a net downward shift of all the levels. For the first and second alkali $^2P_{3/2}$ states, α_2 is negative. The center of gravity of the energy levels in Figs. 1–3 is independent of the electric field value.

C. Calculation of Polarizabilities

From (23) and (24) of Ref. 3 we find that the scalar and tensor polarizabilities of the $P_{3/2}$ states of an alkali atom are

$$\alpha_0 = -\tfrac{2}{45}\left[9D(\tfrac{5}{2}) + D(\tfrac{3}{2}) + 5S(\tfrac{1}{2})\right] , \qquad (9)$$

$$\alpha_2 = \tfrac{2}{225}\left[9D(\tfrac{5}{2}) - 4D(\tfrac{3}{2}) + 25S(\tfrac{1}{2})\right] , \qquad (10)$$

where the terms $S(\frac{1}{2})$ and $D(J)$ account for perturbations from S and D states of the atom. In Eqs. (9) and (10),

$$S(\tfrac{1}{2}) = \sum_{n'} \frac{e^2\left[\int_0^\infty dr\, R(nP_{3/2}) r\, R(n'S_{1/2})\right]^2}{E(nP_{3/2}) - E(n'S_{1/2})} , \qquad (11)$$

$$D(\tfrac{3}{2}) = \sum_{n'} \frac{e^2\left[\int_0^\infty dr\, R(nP_{3/2}) r\, R(n'D_{3/2})\right]^2}{E(nP_{3/2}) - E(n'D_{3/2})} , \qquad (12)$$

$$D(\tfrac{5}{2}) = \sum_{n'} \frac{e^2\left[\int_0^\infty dr\, R(nP_{3/2}) r\, R(n'D_{5/2})\right]^2}{E(nP_{3/2}) - E(n'D_{5/2})} . \qquad (13)$$

The radial wave functions of the electron are $r^{-1}R$. Note that the $S(J)$ and $D(J)$ of this paper are exactly half as large as those of Ref. 3. Also note that there is a transcription error in Eq. (23) of Ref. 3; the coefficients of $S(\frac{1}{2})$ should have been 5 and 25 instead of 10 and 50. However, the correct version of (23) was used in Ref. 3 to calculate the numerical values of the polarizabilities, all of which agree with the calculations of the present paper.

From (9) and (10) we find that the polarizability of the $\pm\frac{3}{2}$ sublevels of a $J = \frac{3}{2}$ state is

$$\alpha(\pm\tfrac{3}{2}) = \alpha_0 + \alpha_2 = -\tfrac{8}{25}D(\tfrac{5}{2}) - \tfrac{2}{25}D(\tfrac{3}{2}) \qquad (14)$$

so that the polarizability of a $\pm\frac{3}{2}$ sublevel is determined only by perturbations from the D states. For

the $\pm\frac{1}{2}$ sublevels the polarizability is

$$\alpha(\pm\tfrac{1}{2}) = \alpha_0 - \alpha_2 = \tfrac{12}{25} D(\tfrac{5}{2}) - \tfrac{2}{225} D(\tfrac{3}{2}) - \tfrac{4}{9} S(\tfrac{1}{2}) \qquad (15)$$

so that both D and S terms contribute to the polarizability of the $\pm\frac{1}{2}$ sublevels.

The numerical values of $S(\frac{1}{2})$, $D(\frac{3}{2})$, and $D(\frac{5}{2})$ were computed using the Bates-Damgaard (BD) method for the radial integrals.[15] The program did not use the tables published by those authors but rather generated new values from the basic formulas. The results of this program were thoroughly checked against the original Bates-Damgaard tables. The energy levels were taken from Moore's tables.[16] The results are listed in Table I, where we have entered the quantities $(\int dr \cdots)^2/\Delta E$ and their sums over n' for the first three $^2P_{3/2}$ states of the stable alkalis. Except in the case of cesium the $D(\frac{3}{2})$ and $D(\frac{5}{2})$ integrals were found to be essentially the same so that only $D(\frac{3}{2})$ is tabulated.

III. MEASUREMENT OF α_2 IN THE $5^2P_{3/2}$ STATE OF K^{39}

A. Apparatus

The apparatus used to measure the differential Stark shifts in the second excited $^2P_{3/2}$ state of K was described previously by Khadjavi *et al.*[3] Briefly, the experimental method is as follows: Resonance radiation from a lamp is focussed onto an atomic beam in a region near the center of a pair of electric field plates. The scattered light is detected by a photomultiplier tube. The polarizations of the incident and detected beams of radiation were chosen to be perpendicular to one another and to the electric field. The applied field is purely electric and the light is plane polarized in the plane defined by the incident and detected light directions. The electric field is normal to that plane and is uniform to within a few percent in the field of view of the optical system.

The electric field was swept by a function generator which fed a triangular wave with a 16-sec period to the high-voltage regulator. The high voltage (HV) was measured with a Sensitive Research Model ESH electrostatic voltmeter and was found to be a linear function of the sweep voltage. Thus, during a measurement, the function generator voltage was usually read at the input to the regulator since the lower voltage there was easier to measure.

The signal from the photomultiplier tube passed through a linear amplifier and was stored in a 1024-channel signal averager (TMC Model 1000). The averager was internally swept in a 16-sec cycle that was synchronized with the HV sweep so that the

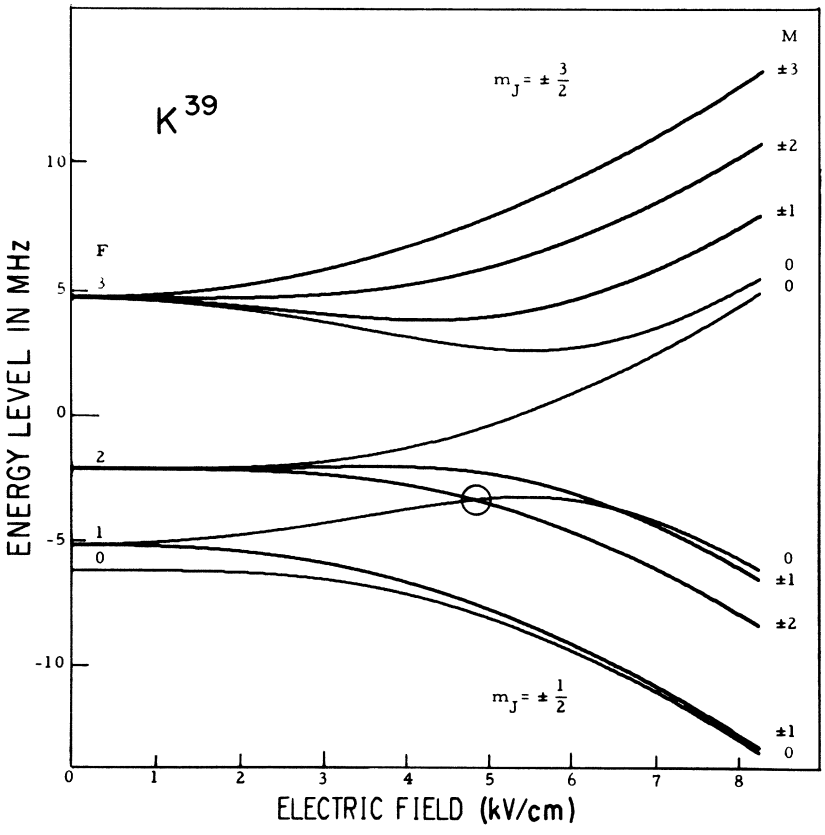

FIG. 2. Same as Fig. 1 for the $5\,^2P_{3/2}$ state of K^{39}, assuming $a = 1.95$ MHz, $b = 0.92$ MHz, $\alpha_2 = -0.260$ MHz/(kV/cm)^2. For the $4\,^2P_{3/2}$ state, multiply the vertical scale by 3.05, the horizontal scale by $0.260/0.024 \cong 10.8$. The single $\Delta m = \pm 2$ crossing which we observed in our measurements is marked with a circle.

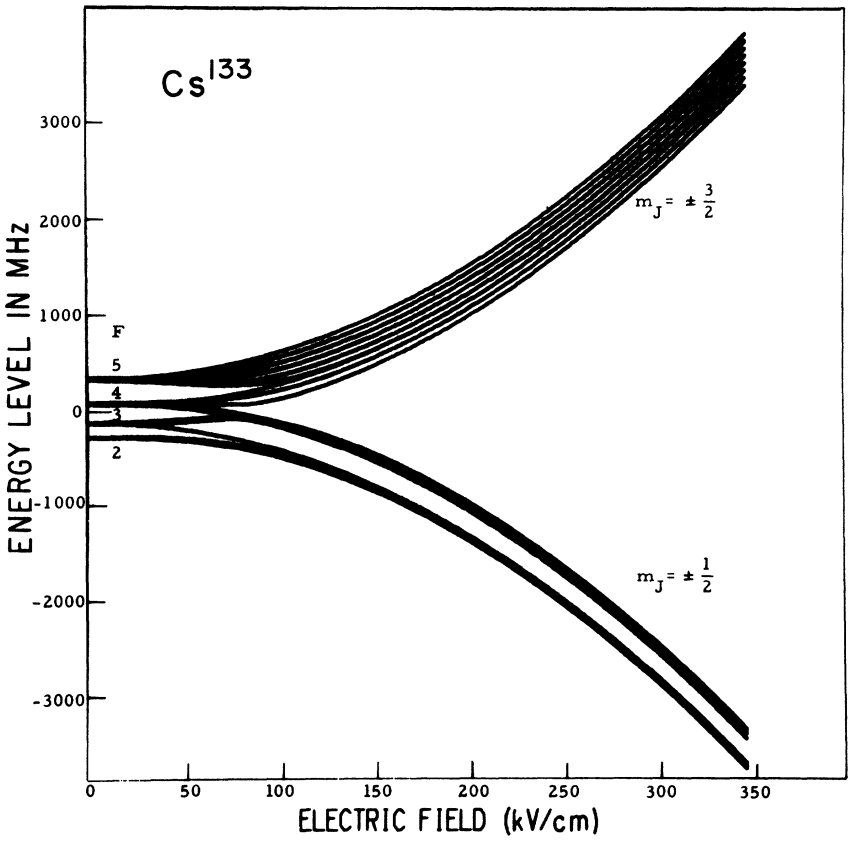

FIG. 3. Same as Fig. 1 for the $6\,^2P_{3/2}$ state of Cs^{133}, assuming $a = 50.67$ MHz, $b = -0.46$ MHz, $\alpha_2 = -0.059$ MHz/(kV/cm)^2.

stored line shape represented intensity vs field. In N sweeps the signal-to-noise ratio of the stored information is increased by $\sqrt{N}$. A typical "run" would consist of several hundred sweeps, or total integration times for each of 1024 points of 5 or 10 sec.

The contents of the averager could be read out onto an X-Y recorder or punched directly onto cards. Normally, both methods were used. After a readout of stored intensity data, a few sweeps were taken using the output of the function generator as input to the averager to obtain a record of the field vs time. Thus, any nonlinearities in $\mathcal{E}(t)$ were unimportant when t was eliminated as a parameter between $\mathcal{E}(t)$ and $I(t)$ to get $I(\mathcal{E})$.

B. Analysis of Data

The experimental data, consisting of a set of intensity values and the corresponding field values, were compared point by point with a theoretically generated set of the same data. The latter set was computed from the Breit formula (see Sec. II B). The calculations require that we know the hyperfine structure and lifetime in the $^2P_{3/2}$ state, and we used the results of Schmieder, Lurio, and Happer,[17] namely, $a = 1.95 \pm 0.05$ MHz, $b = 0.92 \pm 0.1$ MHz, $\tau = 140.8 \pm 1.0$ nsec.

The program that compares the experimental and theoretical data computes their mean square deviation (MSD). The MSD is calculated for a number of theoretical curves which correspond to different values of α_2. The value of α_2 which gives the smallest MSD is quoted as the experimental result.

C. Typical Experimental Data and Results

In Fig. 4 we show a typical experimental line shape as plotted directly from the averager by the X-Y plotter. Although it appears continuous, it actually consists of 1024 separate points. The symmetrical shape is due to the triangular sweep of the field which varies from 8.6 kV/cm at the left to -2.6 kV/cm at the center to 8.6 kV/cm at the right. In the processing of these plots, the symmetrical halves were added together. These data were taken with 470 sweeps, or integration times of about 7.5 sec per point.

The average of α_2 determined from the two best independent experimental runs is

$$\alpha_2(K^{39}5\,^2P_{3/2}) = -0.263 \pm 0.04 \text{ MHz/(kV/cm)}^2 \ .$$

The error limits here represent two standard deviations, or 96% confidence. In Fig. 5 are plotted one set of experimental points and the best-fit theoret-

TABLE I. Values of $[\int_0^\infty R(nJ)r\,R(n'J')dr]^2/[E(nJ)-E(n'J')]\times 10^5$ [(r in Bohr radii, $E(nJ)$ in cm^{-1})].

	Lithium			Sodium			Potassium			Rubidium			Cesium		
	$2\,^2P_{3/2}$	$3\,^2P_{3/2}$	$4\,^2P_{3/2}$	$3\,^2P_{3/2}$	$4\,^2P_{3/2}$	$5\,^2P_{3/2}$	$4\,^2P_{3/2}$	$5\,^2P_{3/2}$	$6\,^2P_{3/2}$	$5\,^2P_{3/2}$	$6\,^2P_{3/2}$	$7\,^2P_{3/2}$	$6\,^2P_{3/2}$	$7\,^2P_{3/2}$	$8\,^2P_{3/2}$
$2\,^2S_{1/2}$	+111														
3	−72	+2890		+107											
4	−93	−8	+9	−210	+2286	+14	+191								
5		−47	−9904	−5	−3590	+18 230	−260	+3581	+17	+207	+2				
6		−10	−308	−1	−61	−25 100	−8	−4178	+26 240	−332	+3736	+25	+255	+2	
7		−4	−65		−12	−355	−2	−85	−28 040	−9	−5170	+26 610	+399	+4397	+30
8		−2	−24		−4	−63		−17	−467	−2	−93	−33 890	−11	+6007	+30 250
9					−2	−22		−6	−85	−1	−18	−494	−2	−108	−38 320
10								−3	−30		−7	−88	−1	−21	−556
11								−2	−14		−3	−31		−8	−98
12								−1	−8					−4	−33
$S(\frac{1}{2})$	−55	+2819	−10292	−110	−1383	−7295	−79	−710	−2384	−137	−1553	−7870	−159	−1748	−8726
$3\,^2D_{3/2}$	−119	−28 770	+56	−280	+7950		−611	+1253	+11						
4	−13	−796	−283 600	−16	−2565	+77 880		−8429	+9885	−839	+456	+11			
5	−4	−96	−3514	−4	−153	−13 040		−12	−54 570	−8	−13 530	+3737	+1524	+22	+1
6		−30	−415	−1	−37	−760			−2	−4	−46	−92 600	−123	−38 110	+409
7		−13	−125		−14	−179				−2	−23	−131	−21	−947	−300 400
8		−7	−55		−7	−69				−1	−10	−65	−7	−142	−4006
9		−4	−30		−4	−35				−1	−6	−32	−3	−47	−555
10											−3	−17	−2	−22	−176
11													−1	−12	−79
$D(\frac{3}{2})$	−139	−29 712	−28 7730	−302	+5169	+63 789	−612	−7190	−44 676	−856	−13 165	−89 094	−1715	−39 256	−304 790
$3\,^2D_{5/2}$															
4															
5													−1524	+25	+1
6													−122	−36 110	+450
7													−21	−885	−279 700
8													−7	−137	−3710
9													−3	−45	−528
10													−2	−21	−170
11													−1	−12	−77
$D(\frac{5}{2})$													−1681	−37 185	−283 760

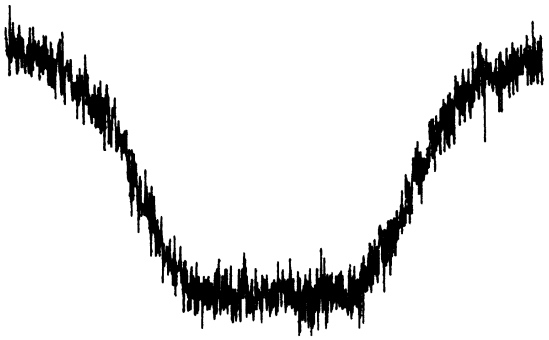

FIG. 4. Typical level-crossing signal for the $5\,^2P_{3/2}$ state of K^{39} as read out by the X-Y plotter directly from the 1024-channel analyzer memory. The electric field varies from 8.6 kV/cm to − 2.6 kV/cm to 8.6 kV/cm, left to right. This symmetrical waveform is due to sweeping the field in a triangular wave. The plot appears continuous, although it is actually 1024 separate points.

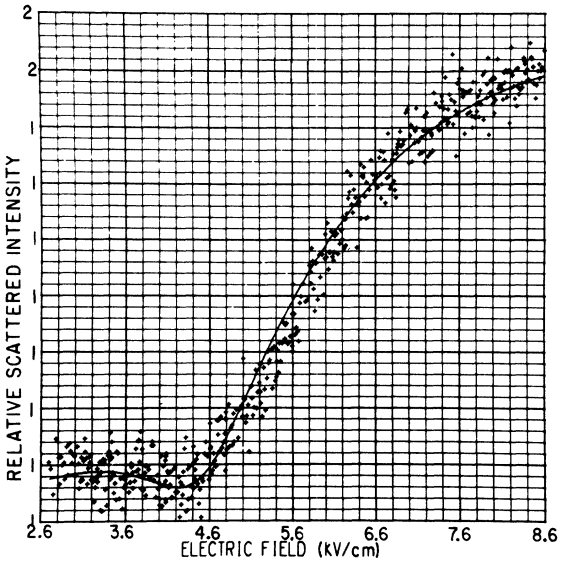

FIG. 5. Experimental points and the best-fit theoretical line shape, which is for α_2 ($K^{39}\,5\,^2P_{3/2}$) = − 0.263 ± 0.04 MHz/(kV/cm)^2.

ical curve. These data show considerably more noise than the data used to determine a and τ.[17] This occurs because the resonance light for exciting the second $^2P_{3/2}$ state is less intense than the light for exciting the first excited state and the photon scattering cross section of the second excited state is smaller than that of the first excited state. Also, the electric field plates both reduce the size of the atomic beam and contribute to increased instrumental scattering.

IV. COMPARISON OF THEORETICAL AND EXPERIMENTAL RESULTS

In Table III we list all the reliable determinations of α_0 and α_2 known to us. Not included are clearly incorrect results, or data that did not permit determining α_0 and/or α_2. The values in this table are plotted in Fig. 6. It should be noted that the

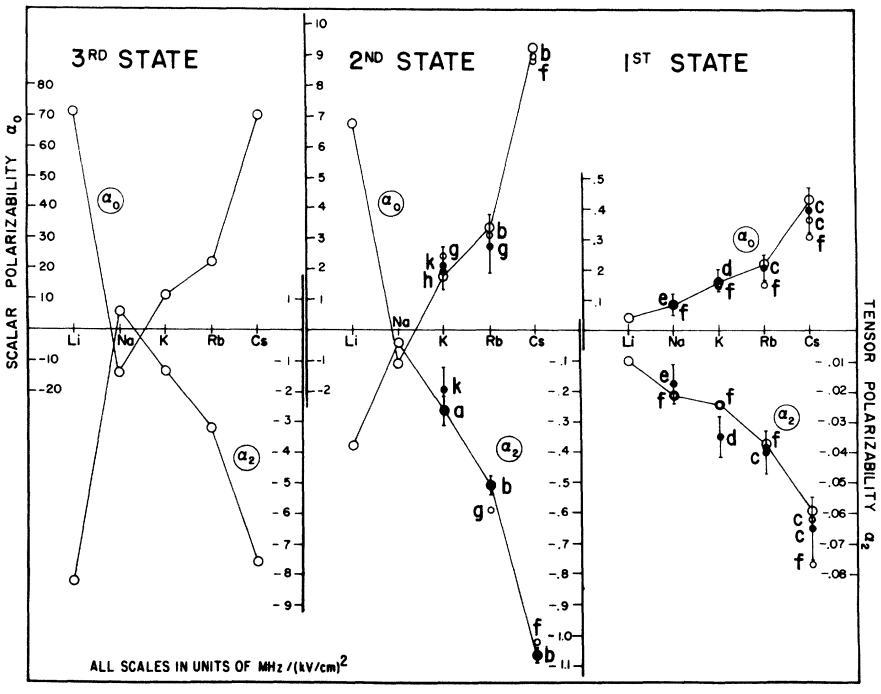

FIG. 6. Comparison of the computed values of α_0, α_2 reported here (Table III) (large open circles), and other theoretical (small open circles) and experimental (small solid circles) results: a, this work; b, Ref. 3; c, Ref. 10; d, Ref. 9; e, Ref. 7; f, Ref. 11; g, Ref. 18; h, Ref. 6; k, Ref. 8.

TABLE II. Scalar and tensor polarizabilities of the $^2P_{3/2}$ states of the alkali atoms.[a]

		Li	Na	K	Rb	Cs
1st	α_0	+ 0.040	+ 0.086	+ 0.158	+ 0.224	+ 0.427
	α_2	− 0.010	− 0.021	− 0.024	− 0.037	− 0.059
2nd	α_0	+ 6.855	− 1.085	+ 1.828	+ 3.377	+ 9.269
	α_2	− 0.377	− 0.042	− 0.260	− 0.507	− 1.072
3rd	α_0	+70.942	−14.568	+11.137	+22.534	+70.299
	α_2	− 8.217	+ 0.662	− 1.375	− 3.111	− 7.523

[a]BD calculation. Units of α_0, α_2, MHz/(kV/cm)^2. Example: $\alpha_2(K^{39}\,5\,^2P_{3/2}) = -0.260$ MHz/(kV/cm)^2.

scales in these plots are related by multiples of 10.

It is clear from Fig. 6 that α_0 and α_2 can be calculated reliably to a few percent using the Bates-Damgaard (BD) method to evaluate the radial integrals. This is reasonable since the largest contribution to the integrals comes from large r, where the Coulomb approximation (BD) method is most valid. The measured values of α_2 for the second $^2P_{3/2}$ states of K, Rb, and Cs all agree with the calculation to within experimental error.

The uncertainty in the theoretical calculations of α_0 and α_2 arises from the radial integrals and from the truncation of the sum over perturbing states. The energies are known experimentally to high accuracy.

V. CONCLUSIONS

Several remarks about our results for the alkali atoms (Tables II and III, Fig. 6) can be made:

(a) The polarizabilities of the alkalis apparently can be calculated within a few percent with the BD method, judging by the agreement with existing measurements. One might thus expect the BD method to be accurate for any atom or ion with a single electron outside of closed shells.

(b) The polarizabilities monotonically increase in absolute value with the atomic number, with the exception of lithium.

(c) The polarizabilities increase as one goes to

TABLE III. Calculated and experimental polarizabilities. References marked with asterisks are from this work. ω_0 and α_2 are in units of MHz/(kV/cm)^2.

Atom	State	α_0 (calc)	α_0 (expt)	α_2 (calc)	α_2 (expt)	Ref.
Li^7	$2\,^2P_{3/2}$	+0.04		−0.01		*
		+0.24		+0.002		11
	$3\,^2P_{3/2}$	+6.855		−0.377		*
	$4\,^2P_{3/2}$	+70.942		−8.217		*
Na^{23}	$3\,^2P_{3/2}$	+0.084		−0.020		11
		+0.086		−0.021		*
			+0.089		−0.017	7
	$4\,^2P_{3/2}$	−1.085		−0.042		*
	$5\,^2P_{3/2}$	−14.568		+0.662		*
K^{39}	$4\,^2P_{3/2}$	+0.156		−0.024		11
		+0.158		−0.024		*
			+0.156 ± 0.03		−0.035 ± 0.006	9
	$5\,^2P_{3/2}$	+1.828		−0.260	−0.263 ± 0.04	*
			+1.95		−0.19	8
			+2.01		−0.70	6
	$6\,^2P_{3/2}$	+11.137		−1.375		*
Rb^{85}	$5\,^2P_{3/2}$	+0.153		−0.039		11
		+0.221	+0.213 ± 0.03	−0.036	−0.040 ± 0.006	10
		+0.224		−0.037		*
	$6\,^2P_{3/2}$	+2.68		−0.58		18
			+2.73		−0.72	6
		+3.2		−1.14		12
		+3.34		−0.494	−0.521 ± 0.021	3
		+3.377		−0.507		*
	$7\,^2P_{3/2}$	+22.534		−3.111		*
Cs^{133}	$6\,^2P_{3/2}$	+0.313		−0.076		11
		+0.372	+0.398 ± 0.06	−0.047	−0.065 ± 0.01	10
		+0.427		−0.059		*
	$7\,^2P_{3/2}$	+8.88		−1.02		11
		+9.03		−1.05	−1.077 ± 0.043	3
		+9.269		−1.072		*
					−0.993 ± 0.02	19
	$8\,^2P_{3/2}$	+70.299		−7.523		*

higher excited states. In fact, for the first three P states the polarizabilities in the $(n+1)$st excited state are roughly ten times those in the nth excited state. Both this effect and (b) arise from the fact that a less strongly bound valence electron is more easily distorted by the field.

(d) The scalar polarizability α_0 is roughly ten times the tensor polarizability α_2. Thus the differential shift among magnetic substates is only about a tenth of the absolute shift of all the substates.

(e) All $\alpha_0 > 0$ and all $\alpha_2 < 0$, except for the higher $^2P_{3/2}$ states of Na, which are strongly perturbed by D states lying at slightly lower energies. Perturbing states tend to repel the perturbed state, so states above the $^2P_{3/2}$ energy tend to depress that level, states below tend to raise it. But since the higher states usually predominate in their contributions to α_0 we generally find that the levels are pushed to lower energy, i.e., $\alpha_0 > 0$. In the case of Na, one D state lies just below the $P_{3/2}$ state, and yields a large negative contribution to α_0.

(f) The S states contribute little to the polarizabilities. This is a fortuitous circumstance that occurs because the $^2P_{3/2}$ states lie roughly midway between the nearest S states, so their contributions to α_0 and α_2 very nearly cancel. This is readily seen in Table I.

ACKNOWLEDGMENTS

The authors are grateful to J. Clendenin for excellent programming assistance and to R. Holohan for excellent laboratory assistance.

*Work supported in part by the Joint Services Electronics Program (U. S. Army, U. S. Air Force, and U. S. Navy) under Contract No. DA-28-043 AMC-00099 (E).

†Present address: Lawrence Radiation Laboratory, Berkeley, Calif. 94720.

‡Present address: IBM Watson Laboratory, Yorktown, N. Y. 10598.

[1]A recent review of the Stark effect has been compiled by A. M. Bonch-Bruevich and V. A. Khodovoi, Usp. Fiz. Nauk 93, 71 (1967)[Soviet Phys. Usp. 10, 637 (1968)].

[2]J. R. P. Angel and P. G. H. Sandars, Proc. Roy. Soc. (London) A305, 125 (1968).

[3]A. Khadjavi, A. Lurio, and W. Happer, Phys. Rev. 167, 128 (1968).

[4]C. Schwartz, Ann. Phys. (N.Y.) 2, 156 (1959).

[5]A. Dalgarno and J. T. Lewis, Proc. Roy. Soc. (London) A233, 70 (1956).

[6]Y. T. Yao, Z. Physik 77, 307 (1932).

[7]H. Kopfermann and W. Paul, Z. Physik 120, 545 (1943).

[8]W. Grotrian and G. Ramsauer, Z. Physik 28, 846 (1927).

[9]R. Marrus and J. Yellin, Phys. Rev. 177, 127 (1969).

[10]R. Marrus, D. McColm, and J. Yellin, Phys. Rev. 147, 55 (1966).

[11]K. Murakawa and M. Yamamoto, J. Phys. Soc. Japan 20, 1057 (1965).

[12]J. G. Kirkwood, Z. Physik 33, 521 (1932).

[13]E. U. Condon, Phys. Rev. 43, 648 (1933).

[14]E. U. Condon and G. H. Shortley, *The Theory of Atomic Spectra* (Cambridge U. P., Cambridge, England, 1953)

[15]D. R. Bates and A. Damgaard, Phil. Trans. Roy. Soc. London 242, 101 (1949).

[16]C. E. Moore, Natl. Bur. Std. (U.S.) Circ. No. 467, Vols. I, II, III (unpublished).

[17]R. W. Schmieder, A. Lurio, and W. Happer, Phys. Rev. 173, 76 (1968).

[18]W. Thoman, Z. Physik 34, 586 (1925).

[19]G. Khvostenko and M. Chaika, Opt. i Spektroskopiya 25, 246 (1968)[Opt. Spectry. (USSR) 25, 450 (1968)].

PHYSICAL REVIEW A VOLUME 3, NUMBER 4 APRIL 1971

Perturbation of a Decaying State*

Richard M. More
Department of Physics, University of Pittsburgh, Pittsburgh, Pennsylvania 15213
(Received 3 August 1970)

One intuitively expects that a long-lived decaying state must have many properties like those of true eigenstates, with interesting technical modifications to encompass the complex energy. We examine here the small change in the complex energy due to the application of a weak perturbation.

Apparently, the energy levels of a quantum system fall into two distinct groups, the discrete and continuous spectra. An intermediate possibility exists, however, which unites some aspects of both. This possibility, which occurs in a wide variety of atomic and nuclear systems, is the decaying state. Here the spectrum is, strictly speaking, continuous; nevertheless a carefully prepared superposition of continuum states behaves, for a time, very much like a discrete eigenstate. To each decaying